AIMS Materials Science, 5(5): 902–915.
DOI: 10.3934/matersci.2018.5.902
Received: 07 June 2018
Accepted: 09 August 2018
Published: 12 September 2018

http://www.aimspress.com/journal/Materials

Research article

Densification behaviour of sintered aluminum composites during hot deformation

Sumesh Narayan[1,*] and Ananthanarayanan Rajeshkannan[2]

[1] Senior Lecturer, Mechanical Engineering, School of Engineering and Physics, Faculty of Science, Technology & Environment, The University of the South Pacific, Laucala Campus, PO Box 1168, Suva, FIJI

[2] Associate Professor, Mechanical Engineering, School of Engineering and Physics, Faculty of Science, Technology & Environment, The University of the South Pacific, Laucala Campus, PO Box 1168, Suva, FIJI

* **Correspondence:** Email: narayan_su@usp.ac.fj; Tel: +6793232034; Fax: +6793231538.

Abstract: In this study, an investigation on the densification behavior and forming limit of powder metallurgy composites containing hard carbide particles were carried out. The selected composite materials are Al4TiC, Al4WC, Al4Fe_3C and Al4Mo_2C. The compacts of 0.82 and 0.86 relative density and 0.4 and 0.6 aspect ratio were prepared on a 1-MN capacity hydraulic press using suitable die-set assembly. Sintering was carried out at 594 ℃ for 60 minutes in an electrical muffle furnace. Hot upsetting was carried out at the sintering temperature immediately after the sintering process and the forming process was stopped once visible cracks were seen on the free surface. Flat dies on the upper and lower surface were employed under dry friction conditions during hot upsetting. Finally, the densification behavior and forming limit of sintered-forged aluminium composite preforms is presented in this research work. It was concretely noted that Al4TiC produced the best density amongst all the above mentioned aluminium composites. Further, it was seen that Al4Mo_2C and Al4WC produced good final height and diameter strain at fracture.

Keywords: densification; forming limit; aluminium composite; hot forging; powder metallurgy

1. Introduction

Powder metallurgy metal matrix composites are extensively employed in industries due to some very important properties such as light weight, good mechanical properties such as fatigue, tensile, impact, rigidity [1] and good chemical properties such as corrosion resistance [2]. These components are commonly used in growing automotive, structural and aerospace industries [3,4]. TiC, SiC and Al_2O_3 reinforced aluminium parts are extensively employed in industry due to many good properties such as low specific density, good wear resistance and low thermal expansion coefficient. SiC reinforced aluminium composites [5,6], TiC reinforced aluminium composites [7] and Al_2O_3 reinforced aluminium composites [8] have shown improved properties in aluminium metal matrix composites such as hardness, tool wear in turning, improvement in wear resistance and reduced corrosion rate. The addition of titanium carbide particles to prepare powder metallurgy (P/M) composite steels showed significant improvements in densification, formability and mechanical properties [9,10]. Further, addition of TiC particles to aluminium foams resulted in increased compressive strength and energy absorption capabilities [11]. Tungsten carbide additions are seen to improve hardness, elastic modulus and wear resistance in tungsten carbide reinforced copper composites [12]. In this research the authors studied reinforcing aluminium metal matrix composites with WC, TiC, Fe_3C and Mo_2C due to its possible industrial uses. WC, Fe_3C and Mo_2C are rarely found in literature as reinforcing particulates; however, the authors believe that these particulates may provide enhanced properties when reinforced in aluminium metal matrix composites and is great significance for industrial applications. Densification behavior plays a key part in the enhancement of the aforementioned properties in the aluminium metal matrix composites. Danninger et al. [13] have reported the correlation between material density, Vickers hardness and tensile strength in sintered powder metallurgy iron and steels specimens. It was reported that the final density achieved by the specimen had great effect on the hardness and tensile properties. Further, it was reported [14,15] that the mechanical properties such as impact, tensile and fatigue properties of powder metallurgy steels are greatly influenced by the relative density, sintering time and temperature. Hence, densification studies are absolute necessary and the necessary changes in the processing techniques can be implemented in the production of such structural parts.

One of the major drawbacks of P/M materials are the pores left in the final part after processing. The porosity present in the final part has significant negative effect on almost all properties of the P/M materials. The pores present in the P/M materials especially the open ones has significant effect on the densification behavior and solving these problems will increase the potential use of P/M parts for industrial applications. Powder preform forging is a secondary deformation method employed to conventionally make P/M parts to achieve the near net final shape enhancing density of the product simultaneously for structural and heavy duty applications. The presence of circumferential mean stress on the free surface plays an important role in densification and pore closure and depends on amount of porosity and friction. Rahimian et al. [16] studied the influence of sintering time and temperature and particle size on the densification behavior as well as other properties. They showed that the particle size and sintering time and temperature has different densification properties and this also affects other properties such as hardness, yield strength, compressive strength and elongation to fracture. Many researchers [7,9,16] evaluated the influence of applied stresses, strain rates and deformations levels to study deformation and densification behavior of P/M materials. Further, experimental investigations are mainly used to study the performance of P/M materials [17–23].

Apart from experimental studies many researchers have used mathematical models and simulations to study densification behavior of P/M materials. The material yield stress plays an important role in achieving the compacted part's final strength and density. A new deformation model was presented [24,25] which included modifying Mohr-Coulomb and work hardening hypothesis which included internal friction, die-wall friction and work hardening during the compaction process. Other factors that also affected the final compacted density were starting density of the compact and the pressure distribution from the center to the edge of the preform for a given friction condition, lubricated powders and higher particle size. Zhou et al. [26] presented a densification mathematical model for porous metallic powder materials. They reported that the plastic deformation of the metallic material is mostly caused by the slipping of crystal lattice. This principle can be used effectively to improve the density and strength in the P/M materials. Further, they introduced voids in the FEM model making it possible to carry out simulations correctly and in a timely manner. Hua et al. [27] presented and validated several yield criterion that are used to study plastic deformation behavior of compressible P/M materials. The proposed yield criterion can predict the initial yield as well as successive yielding point of compressible sintered P/M materials. The effects of initial density and densification strengthening are depicted by the proposed criteria. Because of the presence of pores in the P/M materials, almost all mathematical models have some assumptions and ambiguity.

In view of this and lack of literature found for WC, Fe_3C and Mo_2C reinforced aluminium metal matrix composites motivated to carry out this research work. In this study, the authors attempted to investigate the densification behavior and forming limit of powder metallurgy composites containing hard carbide particles. The selected materials are Al4TiC, Al4WC, Al4Fe_3C and Al4Mo_2C. The secondary forming process induces internal stresses in the powder metallurgy materials and leads to high stress concentration areas due to the presence of internal pores. This phenomenon leads to material failures through initiation of surface cracks, thus it is vital to study the extent by which the material could be deformed so that appropriate die design and processing techniques can be employed to produce parts free from defects.

2. Theoretical analysis

Many researchers have used the following theorem to formulate equation to determine yield strength of powder metallurgy materials

$$\frac{A}{6}\left(2\sigma_\theta^2 + 2\sigma_z^2 - 4\sigma_\theta\sigma_z\right) + B\left(4\sigma_\theta^2 + \sigma_z^2 + 4\sigma_\theta\sigma_z\right) = \delta Y_0^2 \tag{1}$$

where *A*, *B*, δ are yield criterion parameters and are functions of fractional theoretical density and Y_0 is yield strength of a full dense material having fractional theoretical density ρ [28].

Hua et al. [27] explored to find the yield criterion parameters by studying plastic Poisson's ratio, relative density and flow stress of the matrix material. Further, they compared their findings with several yield criterions for sintered powder material by other researchers. The following yield criteria parameters are chosen in this research as $A = 2 + \rho^2$, $B = (1 - \rho^2)/3$, $\delta = [(\rho - \rho_0)/(1 - \rho_0)]^2$. Eq 1 now can be written as

$$Y_0 = \sigma_{eff} = \left[\frac{(1-\rho_0)^2(\sigma_z^2 - 2\sigma_\theta^2 - \rho(\sigma_\theta^2 - 2\sigma_\theta\sigma_z))}{(\rho-\rho_0)^2} \right]^{0.5} \quad (2)$$

Equation 2 gives the expression for equivalent stress in terms of cylindrical coordinates.

Narayansamy et al. [17] stated the hoop stress (σ_θ) under triaxial stress state condition as:

$$\sigma_\theta = \left[\frac{2\alpha + \rho^2}{2 - \rho^2 + 2\rho^2\alpha} \right] \sigma_z \quad (3)$$

where, $\alpha = \frac{d\varepsilon_\theta}{d\varepsilon_z}$.

The stress formability factor [18] is given as

$$\beta = \frac{J_1}{(3J_2^{/})^{0.5}} = \frac{3\sigma_m}{\sigma_{eff}} \quad (4)$$

where, $\sigma_m = \frac{\sigma_r + \sigma_\theta + \sigma_z}{3} = \frac{2\sigma_\theta + \sigma_z}{3}$, is the hydrostatic stress.

The stress formability factor given in Eq 4 highlights the consequence of mean and effective stress on the forming limit of P/M preforms during the deformation process.

Further, the axial strain, diameter strain and hoop strain can be calculated using the basic equations as

$$\varepsilon_z = \ln \frac{h_o}{h_f} \quad (5)$$

$$\varepsilon_d = \ln \frac{D_c}{D_o} \quad (6)$$

$$\varepsilon_\theta = \ln\left(\frac{\left(2D_b^2 + D_c^2\right)}{3D_o^2} \right) \quad (7)$$

where, h_o is the initial height and h_f is the deformed height of the specimen, D_o is the initial diameter, D_c is the average contact diameter of top and bottom surfaces of the deformed specimen and D_b is the bulge diameter.

3. Experimental details

The respective powder compacts used in the present investigation were prepared using 150 μm aluminium powder and 50 μm carbide powders, namely, titanium, tungsten, molybdenum and iron carbide. All powders used in the present investigation had purity levels of 99.7%.

The parameters chosen for this research work are two aspect ratios (AR), 0.4 and 0.6, two initial relative densities (R), 0.82 and 0.86, and four different carbides reinforcement in aluminium. The correct amount of powders were mixed to obtain aluminium 4% by weight titanium carbide composite (Al4TiC), aluminium 4% by weight iron carbide composites ($Al4Fe_3C$), aluminium 4% by weight molybdenum carbide composites ($Al4Mo_2C$) and aluminium 4% by weight tungsten carbide composites (Al4WC) using planetary ball milling machine. The aspect ratio of 0.4 and 0.6 are chosen to understand the effect of geometry on the densification behavior. Further, it is seen that the initial relative density also affects many properties of P/M materials and the safe working initial density are generally above 0.80 [7,9,10]. Hence, two initial relative densities above 0.80 are chosen to see the effect of initial relative density on the densification behavior. The mixing process was carried out for 2 hours at 200 rpm and it was ensured to obtain a homogenized mixture. A consistent apparent density towards the end of the mixing process ensured even distribution of the carbide particles in the matrix.

The required amount of powders to produce compacts having height to diameter ratio of 0.4 and 0.6 and relative density of 0.86 and 0.82 were taken and pressed in a hydraulic press. For each composite material a total of eight compacts are prepared. A compacting pressure of 139 MPa to 159 MPa was enough to produce these compacts. A compressibility graph was produced for each material from which the compacting pressures were determined to produce each compact with specific height and relative density. A paste of Al_2O_3 mixed with acetone was prepared and painted over the compacts to avoid oxidation during the sintering process. The compacts were painted twice with 12 hours of drying period each application.

A further drying process on the ceramic covered compacts was employed at 220 ℃ for 30 minutes in an electric muffle furnace. Then the temperature was increased to the sintering temperature of 594 ℃ and the sintering was carried for further 60 minutes. Each compact was compressively deformed at a temperature of 594 ℃ (sintering temperature) to different levels of height strain in one blow of the hammer. The compacts were placed between two unlubricated dies for open die forging and finally taken for atmospheric cooling. Bulged diameter, contact surface diameter and deformed height together with initial height and diameter of all the compacts were taken and the relative densities of all the compacts were measured using Archimedes principle.

4. Results and discussion

The hard carbide particles which is present in aluminium composite tested here will have some effect on densification. Since the apparent density of the hard carbide particles and its blends as seen in Table 1 are different, the densification and deformation behavior would be different as well as the final density attained would be different. The densification response of carbide reinforced aluminium with relative density and axial strain is shown in Figures 1 and 2. The variables in this study are the initial relative density, 0.82 and 0.86, and initial aspect ratio, 0.4 and 0.6. The relative density of most of the materials continuously improves as the deformation progresses with the reduction of axial height. The densification rate is higher at lower height strain, however, this effect is found to be different in various materials formed in this study. This is because of the larger and higher amount of pores present during the initial stages of deformation which closes with small axial strains. Rudenko et al. [19] also presented similar behavior while studying aluminium metal matrix composite via cold deformation. Generally, it is seen that TiC reinforced aluminium shows better

densification rate when compared to other composites. Al4TiC showed better densification rate at lower height strain, followed by Al4Fe_3C and Al4Mo_2C. Lowest densification rate was obtained by Al4WC composites. As seen in Table 1, the amount of TiC powder required is more to form Al4TiC when compared to the amount of WC powder required to form Al4WC composite. Further, aluminium particles are bigger in size (150 μm) in comparison to carbide particles (50 μm). This means that the powder stacking will be better in Al4TiC compared to other composite. Also the percentage of pores is same in all the composites; however, smaller pores are present in Al4TiC composite. These will aid in densification process, hence, better densification is observed for TiC containing composites. Shear modulus plays an important role in plastic deformation of metals. Shear modulus in metals usually ranges from 20000 to 150000 MPa, however, the shear stress required for plastic deformation are always lower when compared with shear modulus values of that material. As the shear modulus are usually high in metals it is difficult to balance with smaller shear stress required for plastic deformation. Further, shear modulus is directly proportional to shear strength ($T_m = G/2\pi$; where T_m is the shear strength and G is the shear modulus). From Table 1, it can be seen that the shear modulus of WC is much greater than shear modulus of TiC, hence the relative density is lower in Al4WC when compared to Al4TiC. In many materials, dislocation is the carrier of plastic deformation and the energy required to move them is less than the energy required to fracture the material. Later, a steady state densification is observed of all the composites. During this time the densification rate is lower as compared to the initial stage. As the deformation progresses the material increases in strength as a result of reduction of pores thereby increasing in relative density. The pore closure rate is directly proportional to densification; hence, even though the height strain is prominent at the final stage, the densification rate is low. The main reason here is that the cylindrical pores elongate in the lateral direction with the flow of material which is perpendicular to the direction of load application. Similar findings are reported by Narayan and Rajeshkannan [20]. As the deformation progresses the relative density, grain boundary growth and the strength of the material improves. To further improve the relative density by eliminating more pores is difficult as the mobility of the particles decrease due to the improvement in relative density, strength and grain boundary growth for every stage of deformation. Thus the densification rate reduces significantly during the final stages of deformation. Al4TiC showed better densification at final stages of deformation (Figure 1). Similar findings and outcomes were presented by Narayan et al. [20,21].

Further, the effect of aspect ratio and initial relative density is highlighted here. Smaller aspect ratio preform showed better densification rate for all the composites. Further, for Al4TiC smaller aspect ratio preform also had the higher final density attainment, however, for all other composites the final density attainment is almost same irrespective of aspect ratio. The number of pores present in the higher aspect ratio preform is more than the number of pores present on the smaller aspect ratio preform. Hence, the densification rate is higher in smaller aspect ratio preform. Further, when the initial relative density is lower the final density achieved by all the composites are lower compared to higher initial relative density preforms. More number of pores is present in lower initial relative density preform and the chances of crack initiation will be more in lower initial relative density preform compared to higher relative density preform. This could be the cause for low final density attainment by lower initial relative density preform as chances of crack initiation before good final density attainment is highly possible. Similar finding are presented by Narayanasamy et al. [7].

Table 1. Properties of respective powders and its blend.

Properties		Powder/Blend								
		Al	TiC	Fe_3C	Mo_2C	WC	Al4TiC	$Al4Fe_3C$	$Al4Mo_2C$	Al4WC
Density (g/cc)		2.70	4.90	7.70	8.90	15.80	2.79	2.90	2.95	3.23
Shear modulus (GPa)		-	188	-	-	270	-	-	-	-
Apparent density (g/cc)		1.091	-	-	-	-	1.186	1.308	1.325	1.345
To prepare 200 g of Al4xx	Mass (g)	192	8	8	8	8	-	-	-	-
	Volume (cm^3)	71.11	1.63	1.04	0.90	0.51	-	-	-	-

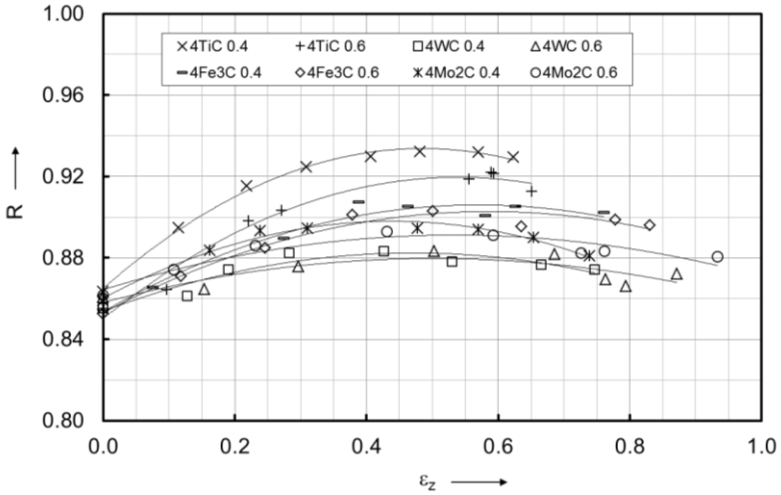

Figure 1. Correlation of R and ε_z for initial relative density of 0.86 [29].

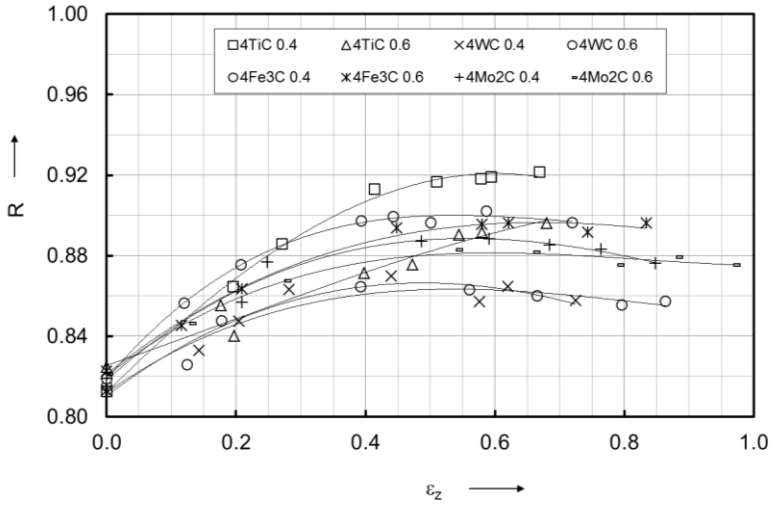

Figure 2. Correlation of R and ε_z for initial relative density of 0.82.

Figures 3 and 4 give that response of hydrostatic stress against axial strain. The variables in this study are the initial relative density, 0.82 and 0.86, and initial aspect ratio, 0.4 and 0.6. It is important

to study hydrostatic stress against axial strain to depict densification behavior of the selected composites. The strength of the P/M material increases with the increasing density, hence, a higher applied load is required to further deform the P/M material each time [22]. In general all the graphs follow similar trend. The hydrostatic stress increase at a higher rate as the material density increases and then it follows a steady state rate. During the initial stage (0 to 0.4 height strain) a higher hydrostatic stress is required to overcome the yield stress of the P/M materials plastic deformation. During this time the larger number of pores present closes increasing the strength and density of the material thereby increasing the load requirements. During the later stages (after 0.4 height strain) of deformation the densification rate is low meaning the effective closure of pores is slow. The cylindrical pores elongate extensively before it is eliminated are the reason for steady state stress requirements during later stages when compared to initial stage [23].

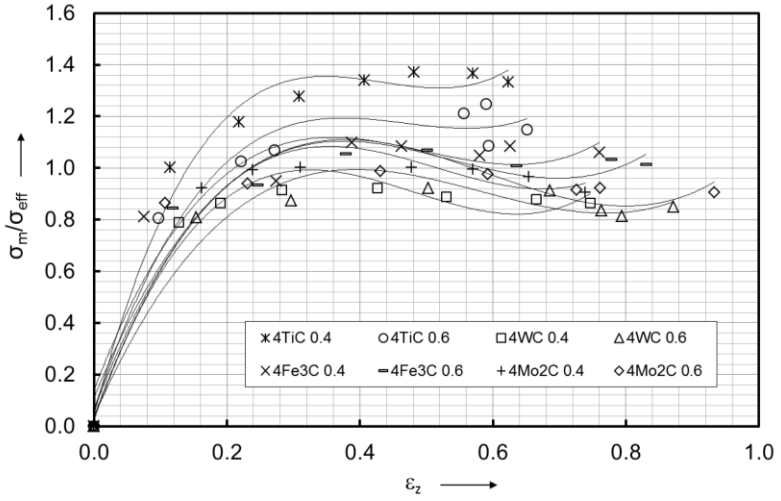

Figure 3. Correlation of σ_m / σ_{eff} and ε_z for initial relative density of 0.86 [29].

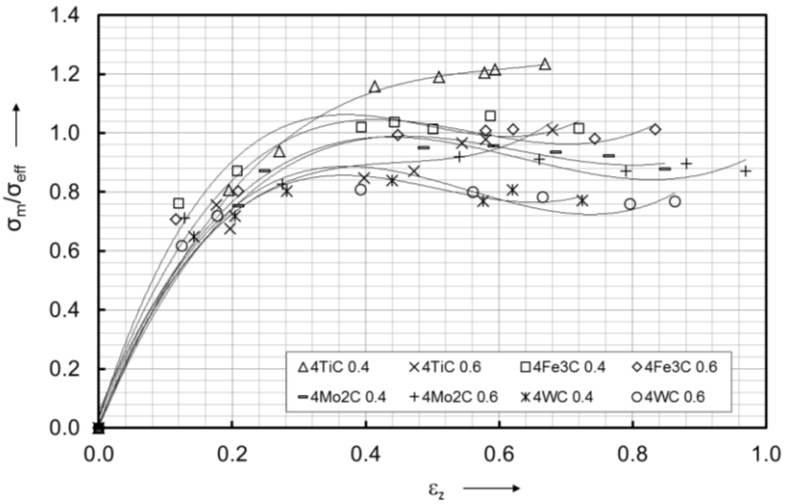

Figure 4. Correlation of σ_m / σ_{eff} and ε_z for initial relative density of 0.82.

From Figures 3 and 4, it is evident that during the initial stage Al4TiC showed higher hydrostatic stress, followed by Al4Fe_3C and Al4Mo_2C and lowest stress found in Al4WC. The same is true during the later stage. Hydrostatic stress mainly due to the friction between the die and contact surfaces of the specimen plays significant role in pore closure. Hence, more hydrostatic stress, more lateral flow of the material and more densification achieved by the material. The hydrostatic force depends on porosity, material property and friction condition between tool and work-piece interface. Further, the effect of initial relative density and aspect ratio is discussed here. Lower aspect ratio and higher initial relative density preform showed better hydrostatic stress when compared to higher aspect ratio preform and lower initial relative density preform, respectively. Hence, more pore closure in lower aspect ratio preform and higher initial relative density preforms. This leads to more densification for these preform as seen in Figures 1 and 2.

For high strength applications of P/M parts for industrials applications the strength in the final part needs to be greater than what is available after primary P/M manufacturing process. It is proved that as the density increases in the P/M parts the final strength of the part also increases. Apart from reinforcing the P/M materials with other high strength materials to increase strength one can increase the density to achieve the high strength of P/M parts. Density in the P/M parts can be increased by secondary processes such as one carried out in this experiment. One of the major drawbacks during the secondary process is the crack appearing at the visible surfaces. This is due to the pores present in the material some of which is closed in turn increasing the density but some may appear as crack. In view of this the forming limit is analyzed.

Figures 5 and 6 give the height strain at fracture for respective composites with initial relative density of 0.82 and 0.86.

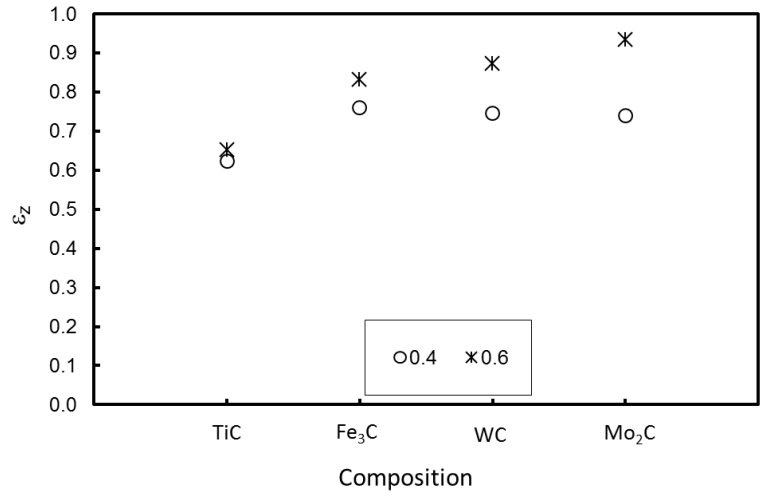

Figure 5. Correlation of fracture height strain (ε_z) and composition for initial relative density of 0.86.

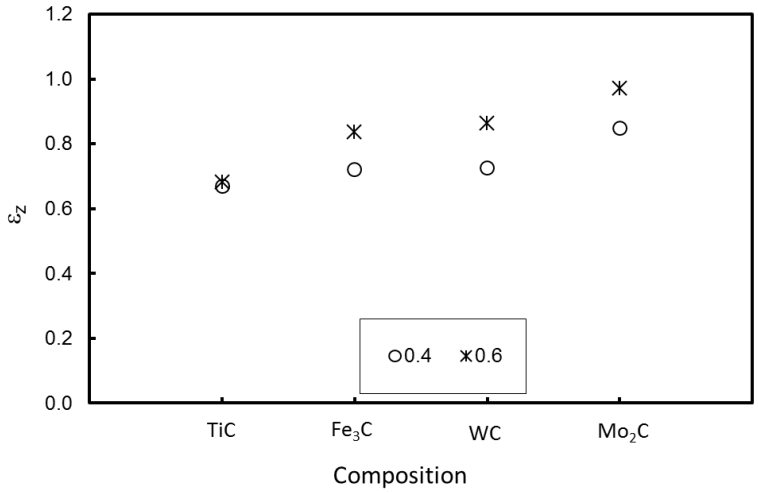

Figure 6. Correlation of fracture height strain (ε_z) and composition for initial relative density of 0.82.

Further, Figures 7 and 8 highlight the relationship between height strains at fracture against diameter strain at fracture for initial relative density of 0.82 and 0.86. It can be seen that Al4Mo_2C has the highest height strain at fracture followed by Al4WC, Al4Fe_3C and lowest for Al4TiC. Further, it can be seen that higher aspect ratio preforms gives better height strain at fracture compared to lower aspect ratio preforms. Further, from Figures 7 and 8, it can be depicted that for composites having lower height strain has lower diameter strain as well as in comparison to other composites. As the height stain improves the diameter strain also improves in the aluminium composites tested in this work. These data can be properly utilized in selecting the forming parameters and procedures. Further, the data can be effectively utilized in die design.

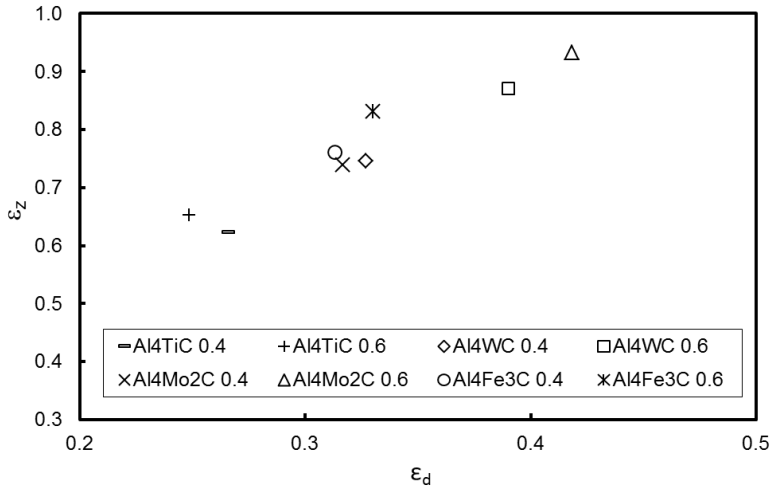

Figure 7. Relationship between fracture height strain (ε_z) and fracture diameter strain (ε_d) for initial relative density of 0.86.

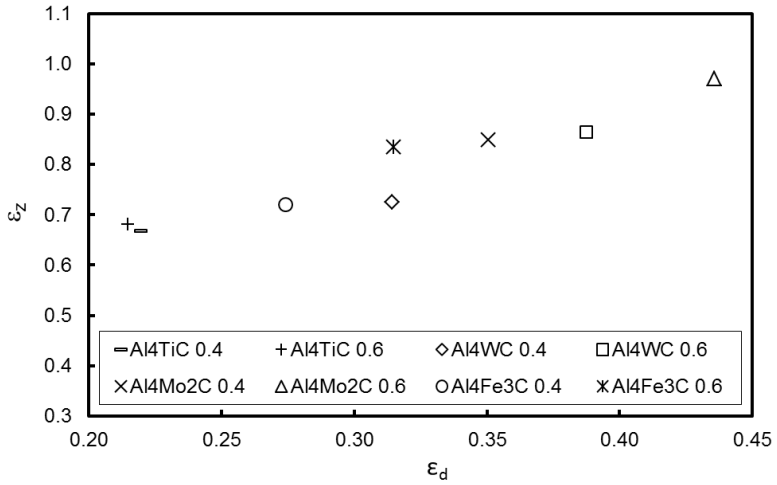

Figure 8. Relationship between fracture height strain (ε_z) and fracture diameter strain (ε_d) for initial relative density of 0.82.

Figures 9 and 10 show the microstructural view of the respective composites used in this research work at 0.86 initial relative density (magnification of 100×). Further, Figure 9 gives the microstructural views at the center of the specimen and Figure 10 gives the microstructural view at the edge of the specimen. The upsetting axis is horizontal in Figures 9 and 10.

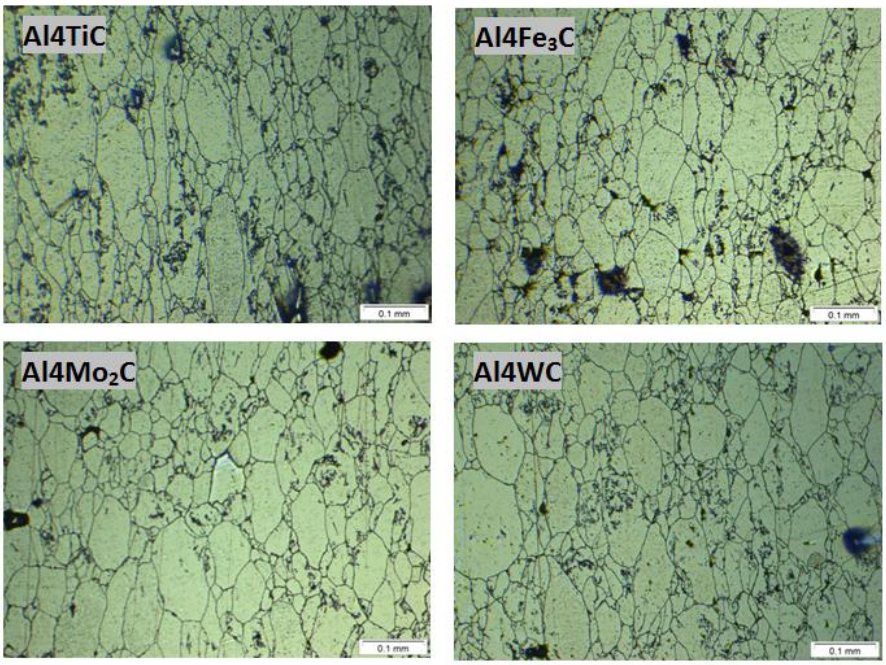

Figure 9. Optical micrographs of various sintered aluminium composites at the center of the specimen.

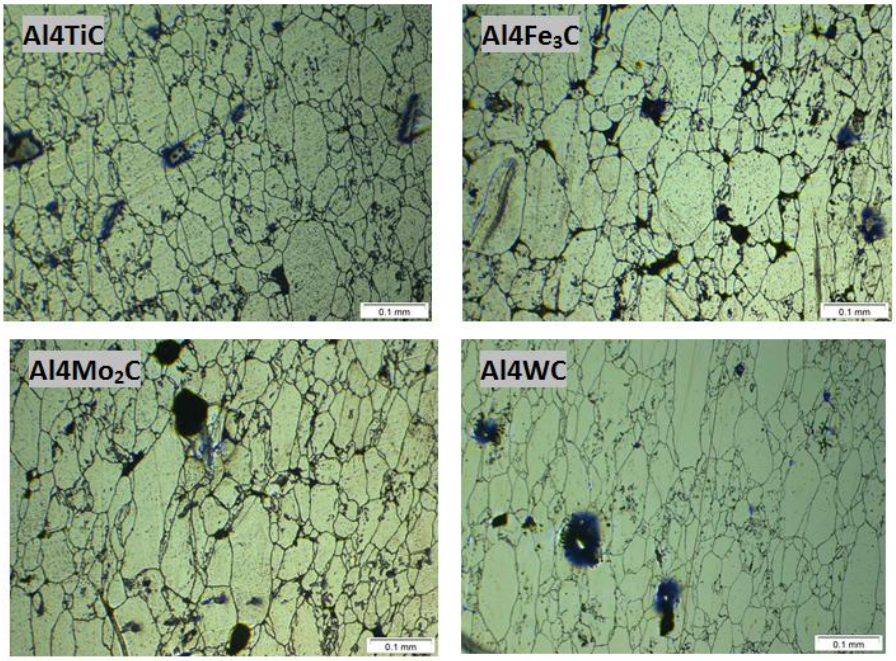

Figure 10. Optical micrographs of various sintered aluminium composites at the edge of the specimen.

Less number of pores is found in the center of the specimen in comparison to the number of pores present at the edge of the specimen. Further, the pores in the center of the specimen are found to be generally smaller in size then the pores at the edge of the specimen. Similar findings are reported by Narayan and Rajeshkannan [30]. Also the pores appear to be round in shape at the center of the specimen while generally elongated towards the edge of the specimen. These behaviors are found for all the composites. Round and spherical pores do not act as stress risers during application and are assumed to be second phase particles [23]. On the other hand, the elongated pores will appear as cracks when further deformation is employed or may undergo further elongation. This will act as stress risers in actual application and cause failures. Hence, these micrographs can be used effectively to employ repressing activities during forging or help in die design so that round or spherical pores are left in the final part or the pores are prevented to appear as cracks and are contained within the bulk material.

5. Conclusions

The forming limit and densification behaviors of Al-4TiC, Al-4WC, Al-4Fe_3C and Al-4Mo_2C were studied in this research work. The findings are as follows:

- The characteristic nature of the densification curves is similar irrespective of the selected compositions, aspect ratio and initial relative density. Al4TiC was found to have the highest final density followed by Al4Fe_3C, Al4Mo_2C and lowest for Al4WC. Further, the effect of aspect ratio and initial relative density became less prominent during the final stages of deformation.
- Al4Mo_2C and Al4WC have the highest height strain and diameter strain at fracture compared to Al4Fe_3C and Al4TiC. Also higher aspect ratio preforms showed higher height and diameter

strain at fracture. The effect of initial relative density on diameter strain and height strain at fracture was almost negligible for these composites.

- Pores found at the center of the specimen were generally lesser in numbers, smaller in size and round in shape. On the other hand, pores at the edge of the specimens were mainly elongated in the direction of deformation. These behaviors are found for all the composites. The extent of pores and grain structure varies extensively in the composites. The final grain distribution conveys strong alignment along the upsetting direction, causing a fiber structure.

Conflict of interest

The authors declare that there is no conflict of interests regarding the publication of this article.

References

1. Kok M (2005) Production and mechanical properties of Al_2O_3 particle-reinforced 2024 aluminium alloy composites. *J Mater Process Tech* 161: 381–387.
2. Torres B, Lieblich M, Ibanez J, et al. (2002) Mechanical properties of some powder metallurgy aluminide and silicide reinforced 2124 aluminium matrix composites. *Scripta Mater* 47: 45–49.
3. Davis G (2012) Design and material utilization, In: Davis G, *Materials for automobile bodies*, London: Butterworth Heinemann, 17–91.
4. Gururaja MN, Rao ANH (2012) A review on recent applications and future prospectus of hybrid composites. *Int J Soft Comput Eng* 1: 352–355.
5. Sahin Y (2003) Preparation and some properties of SiC particle reinforced aluminium alloy composites. *Mater Design* 24: 671–679.
6. Eslamian M, Rak J, Ashgriz N (2008) Preparation of aluminium/silicon carbide metal matrix composites using centrifugal atomization. *Powder Technol* 184: 11–20.
7. Narayanasamy R, Senthilkumar V, Pandey KS (2007) Effect of titanium carbide particle addition on the densification behaviour of sintered P/M high strength steel preforms during cold upset forming. *Mat Sci Eng A-Struct* 456: 180–188.
8. Zhang XQ, Peng YH, Li MQ, et al. (2009) Study of workability limits of porous materials under different upsetting conditions by compressible rigid plastic finite element method. *J Mater Eng Perform* 9: 164–169.
9. Senthilkumar V, Narayanasamy R (2008) Influence of titanium carbide particles addition on the forging behaviour of powder metallurgy composite steels. *P I Mech Eng B-J Eng* 222: 1333–1345.
10. Gopalakrishnan S, Murugan N (2011) Prediction of tensile strength of friction stir welded aluminium matrix TiC particulate reinforced composite. *Mater Design* 32: 462–467.
11. Asavavisithchai S, Opa A (2010) Effect of TiC particles on foamability and compressive properties of aluminium foams. *Chiang Mai J Sci* 37: 213–221.
12. Yusoff M, Othman R, Hussain Z (2011) Mechanical alloying and sintering of nanostructured tungsten carbide-reinforced copper composite and its characterization. *Mater Design* 32: 3293–3298.
13. Dannininger H, Gierl C, Salak A (2009) Relationship between apparent hardness and tensile strength in P/M iron and steels sintered at standard temperatures. *Powder Metall Prog* 9: 1–13.

14. Danninger H, Jangg G, Weiss B, et al. (1993) Microstructure and mechanical properties of sintered iron. I: Basic consideration and review of literature. *Powder Metall Int* 25: 111–117.
15. Danninger H, Jangg G, Weiss B, et al. (1993) Microstructure and mechanical properties of sintered iron. II: Experimental study. *Powder Metall Int* 25: 219–223.
16. Rahimian M, Ehsani N, Parvin N, et al. (2009) The effect of particle size, sintering temperature and sintering time on the properties of Al–Al_2O_3 composites, made by powder metallurgy. *J Mater Process Tech* 209: 5387–5393.
17. Narayanasamy R, Ramesh T, Pandey KS (2005) Some aspects on workability of aluminium–iron powder metallurgy composite during cold upsetting. *Mat Sci Eng A-Struct* 391: 418–426.
18. Rahman MA, El-Sheikh MN (1995) Workability in forging of powder metallurgy compacts. *J Mater Process Tech* 54: 97–102.
19. Rudenko N, Laptev A (2011) Compaction and properties of highly porous powder parts produced with various pore formers. *Mech Test Diagn* 1: 82–87.
20. Narayan S, Rajeshkannan A (2011) Densification behavior in forming of sintered iron–0.35% carbon powder metallurgy preform cold upsetting. *Mater Design* 32: 1006–1013.
21. Rajeshkannan A, Narayan S (2009) Strain hardening behavior in sintered Fe–0.8%C–1.0%Si–0.8%Cu powder metallurgy preform during cold upsetting. *P I Mech Eng B-J Eng* 223: 1567–1574.
22. Raj APM, Selvakumar N, Narayanasamy R, et al. (2013) Experimental investigation on workability and strain hardening behaviour of Fe–C–Mn sintered composites with different percentage of carbon and manganese content. *Mater Design* 49: 791–801.
23. Rajeshkannan A, Rai NS, Chand M, et al. (2014) Densification behavior of sintered-forged aluminium composite preforms. *P I Mech Eng B-J Eng* 228: 441–449.
24. Al-Qureshi HA, Galiotto A, Klein AN (2005) On the mechanics of cold die compaction for powder metallurgy. *J Mater Process Tech* 166: 135–143.
25. Al-Qureshi HA, Soares MRF, Hotza D, et al. (2008) Analyses of the fundamental parameters of cold die compaction of powder metallurgy. *J Mater Process Tech* 199: 417–424.
26. Zhou ZY, Chen PQ, Zhou WB, et al. (2002) Densification model for porous metallic powder materials. *J Mater Process Tech* 129: 385–388.
27. Hua L, Qin X, Mao H, et al. (2006) Plastic deformation and yield criterion for compressible sintered powder materials. *J Mater Process Tech* 180: 174–178.
28. Lewis RW, Khoei AR (2001) A plasticity model for metal powder forming processes. *Int J Plasticity* 17: 1659–1692.
29. Narayan S, Rajeshkannan A (2017) Studies on formability of sintered aluminium composites during hot deformation using strain hardening parameters. *J Mater Res Technol* 6: 101–107.
30. Narayan S, Rajeshkannan A (2016) Workability studies of sintered aluminium composites during hot deformation. *P I Mech Eng B-J Eng* 230: 494–504.

AIMS Press